Laboratory Investigation (2006) 86, 1243–1260

www.laboratoryinvestigation.org

Early pathogenic events associated with Sjögren's syndrome (SjS)-like disease of the nod mouse using microarray analysis

Smruti Y Killedar[1,*], Sarah E Eckenrode[2], Richard A McIndoe[2], Jin-Xiong She[2], Cuong Q Nguyen[1], Ammon B Peck[1,3,4] and Seunghee R Cha[5]

[1]*Department of Oral Biology, College of Dentistry, University of Florida, Gainesville, FL, USA;* [2]*Center for Biotechnology & Genomic Medicine, Medical College of Georgia, Augusta, GA, USA;* [3]*Department of Pathology, Immunology & Laboratory Medicine, College of Medicine, University of Florida, Gainesville, FL USA;* [4]*Center for Orphan Autoimmune Diseases, College of Dentistry, University of Florida, Gainesville, FL, USA and* [5]*Department of Oral & Maxillofacial Surgery, College of Dentistry, University of Florida, Gainesville, FL, USA*

Recently, we reported development of the C57BL/6.NOD-*Aec1Aec2* mouse carrying two genetic intervals derived from the NOD mouse. These two genetic regions confer full Sjögren's syndrome (SjS)-like disease in SjS-non-susceptible C57BL/6 mice. The current study was undertaken to apply microarray technology to define the molecular basis underlying onset of SjS-disease in C57BL/6.NOD-*Aec1Aec2* mice. Using oligonucleotide microarrays, gene expression profiles of submandibular glands derived from 8- to 12-week-old C57BL/6.NOD-*Aec1Aec2* mice and 8-week-old C57BL/6 mice were performed for comparison. Significant differential expressions were determined using the Mann–Whitney *U* test. Hybridizations using submandibular cDNA probes revealed 75 differentially expressed genes at 8 weeks and 105 differentially expressed genes at 12 weeks of age in C57BL/6.NOD-*Aec1Aec2* mice compared to 8-week-old C57BL/6 mice. These genes were related generally to basic cellular activities such as transcription, translation, DNA replication, and protein folding. During the predisease phase, genes upregulated encode proteins associated with the IFN-gamma signal-transduction-pathway (*Jak/Stat1*), TLR-3 (*Irf3* and *Traf6*) and apoptosis (*casp11* and *casp3*), indicative of chronic proinflammatory stimuli, especially IL-1. Between 8 and 12 weeks of age, sets of clustered genes were upregulated that are associated with adaptive immune responses, especially B cell activation, proliferation and differentiation (*Baffr*, *Taci*, *Bcma*, *Blys*, *April*, *CD70*, *CD40L*, *Traf1*, *Traf3*, *Pax5*, *c-Jun*, *Elk1* and *Nf-kB*), and neural receptors (*Taj/Troy*). Altered gene expressions of TLR3 and TNF-superfamily-receptors and ligands during this early phase of SjS suggest a possible viral etiology in the altered glandular homeostasis with an upregulated, possibly overstimulated, B-lymphocyte activation in the early autoimmune response present in the submandibular glands. The importance of NF-κB as a critical signal transduction pathway is also suggested but its link is not yet clear.
Laboratory Investigation (2006) **86,** 1243–1260. doi:10.1038/labinvest.3700487; published online 30 October 2006

Keywords: Sjögren's syndrome; microarray; autoimmunity; NOD mouse; salivary gland

Sjögren's syndrome (SjS) is an autoimmune disease initially targeting primarily the salivary and lacrimal glands, resulting in dry mouth (xerostomia sicca) and/or dry eye (keratoconjunctivitis sicca) disease, respectively.[1] While numerous mouse strains have been developed to study SjS, the NOD mouse has become one of the more extensively characterized for investigating the pathogenesis of autoimmune exocrinopathy.[2–8] Our analyses indicate that NOD mice exhibit loss of saliva flow (up to 75%) and tear flow (up to 35%) by 16–24 weeks of age[9,10] concomitant with leukocyte infiltration of the glands, and this contrasts with other strains such as the NFS/sld mutant mouse thymectomized 3 days after birth or the BAFF transgenic mouse which exhibit salivary dysfunction at much older ages (Ishimaru *et al*,[11] Groom *et al*,[12] respectively) and

Correspondence: Professor SR Cha, DDS, PhD, Department of Oral & Maxillofacial Surgery, College of Dentistry, University of Florida, PO Box 100416, Gainesville, FL 32610, USA.
E-mail: SCHA@dental.ufl.edu
*Current address: The Johns Hopkins Asthma & Allergy Center, 5501 Hopkins Bayview Circle, Rm 2A 58, Baltimore, MD 21224, USA
Received 2 August 2006; revised and accepted 14 September 2006; published online 30 October 2006

often independently of leukocyte infiltration of the exocrine glands. In addition, NOD mice undergo multiple immunopathological changes between 12 and 20 weeks of age, including increases in proinflammatory cytokines, autoantibody production, and levels of acinar cell apoptosis, which closely resemble the disease characteristics in human patients.[9,10,12]

Interestingly, these pathological changes observed in NOD mice appear to occur as a consequence of altered glandular homeostasis.[13,14] Aberrant proteolytic activity, elevated apoptosis, downregulated epidermal growth factor (EGF) gene expression, and reduced amylase activity are commonly observed in NOD mice prior to or during disease onset around 8–10 weeks of age. Although what drives these alterations remains unknown, this altered glandular homeostasis could explain why autoreactive T-cells develop responsiveness against exocrine gland cells in this systemic autoimmune disorder.[7,13] Thus, the NOD mouse model of SjS has given rise to the concept that autoimmune exocrinopathy develops in two phases.[3,5,7,13–17] The initial phase is lymphocyte-independent and occurs as a consequence of intrinsic problems in exocrine tissue homeostasis or differentiated function, potentially associated with delayed-expression of self-antigens or exposure of cryptic/neo antigens. The second phase involves a subsequent tissue specific immunological attack by activated T-cells, B-cells and their products against corresponding self-antigens that leads to SjS-like autoimmune exocrinopathy in the target organs.[18–20]

Studies using NOD mice, considered the best animal model of type I diabetes (T1D), have identified several diabetogenic genetic regions on different chromosomes, referred to as *Idd* susceptibility genes, that determine genetic susceptibility to development of T1D.[21,22] Our previous studies that screened for *Idd* genes responsible for development of SjS-like disease in NOD mice indicated that two genetic intervals, one containing the *Idd5* locus on chromosome 1 and the other containing the *Idd3* locus on chromosome 3, control the physiological aberrations and immunological responses, respectively.[2,23] At the same time, no role for *Idd1*, containing the MHC locus *H-2*^{g7} could be identified. Subsequent studies showed that *Idd3* and *Idd5,* when placed into C57BL/6 mice, were both necessary and sufficient to permit full development of a SjS-like disease. This new SjS-susceptible strain is designated C57BL/6.NOD-*Aec1Aec2*, where *Aec1* corresponds to *Idd3* and *Aec2* corresponds to *Idd5*.[23]

Our previous studies defining the SjS-like disease in NOD mice have focused primarily on the role of individual molecules through the use of gene knockout (KO) mice. While the information obtained from such experiments is ideal for uncovering possible roles of these individual molecules in the disease process, such an approach is less than optimal for discovering new genes or molecular networks involved in the development and onset of disease. In the present studies, we have taken advantage of microarray technology to screen large numbers of genes in order to identify those that are differentially expressed temporally in submandibular glands of the newly generated C57BL/6.NOD-*Aec1Aec2* mouse relative to the nonautoimmune C57BL/6 parental mouse. Use of C57BL/6.NOD-*Aec1Aec2* mice permits comparison with its parental, non-diseased C57BL/6 mice, thereby eliminating differentially expressed genes due to very different genetic backgrounds, for example, in a comparison of NOD *vs* a control strain.

Materials and methods

Animals

C57BL/6J and C57BL/6.NOD-*Aec1Aec2* mice were bred and maintained under SPF conditions within Animal Care Services at the University of Florida, Gainesville. The animals were maintained on a 12 h light–dark schedule and provided water and food *ad libitum*. For this study, female mice were euthanized at either 8 or 12 weeks of age. Both breeding and use of these animals were approved by the University of Florida, IACUC.

Detection of Differentially Expressed Genes using Microarray Analyses

Hybridizations were carried out using MWG Mouse 30 K A Arrays (MWG Biotech, NC, USA) containing 10 752 genes. Microarray slides were produced in-house using epoxy-coated slides printed by the MicroGrid TAS II Biorobotics system (Genetix USA Inc., Boston, MA, USA). Total RNA was isolated from the submandibular glands freshly extracted from individual C57BL/6.NOD-*Aec1Aec2* ($n=5$) and C57BL/6J ($n=5$) mice at either 8 or 12 weeks of age using the RNeasy Mini-Kit (Qiagen, Valencia, CA, USA), as per the manufacturer's protocol. Reference RNA was prepared by combining equal quantities of total RNA from the submandibular glands of C57BL/6J mice ($n=8$) at 8 weeks of age. The 3DNA Array 350kit (Genisphere Inc., Hatfield, PA, USA) was then used to create the hybridization probes from 500 ng of total RNA for each C57BL/6.NOD-*Aec1Aec2* mouse (labeled with Cy3) and each parental C57BL/6J mouse (labeled with Cy5). Each Cy3-labeled sample probe was combined with an equal quantity of the Cy5-labeled reference probe and hybridized to a printed array for 16 h at 42°C. The slides were then washed, dried by centrifugation, and placed in the dark to avoid exposure to light until scanned. Hybridizations were repeated three times for each RNA sample to improve the accuracy of the measurements.

Data Acquisition

An Affymetrix 428™ Scanner (Affymetrix, Santa Clara, CA, USA) was used to create the images by scanning the slide twice, the first time at 532 nm and the second time at 635 nm. This process generated two 16-bit tagged image file format (TIFF) image files. Numerical values for each spot were extracted from the images using MolecularWare (MolecularWare, Cambridge, MA, USA). A statistical program was used to identify/flag spots with low-intensity/background ratios. This flagging procedure allowed, first, a determination of the data quality for each spot (gene) as being sufficiently good to warrant subsequent analysis, and second, elimination of unreliable elements with expression statistically too similar to the background. After 'flagging', the data were uploaded to a flat file database, where the gene expression information was linked to the coordinates of the spot on the array.

Statistical Analyses

For each RNA sample, the medians of the replicates were determined and used to determine the ratios of expression ($\log_2$). Subsequent statistical analyses were based on these median values. The Student's *t* test was used to identify genes with the highest discrimination power between the comparative groups. On first pass, genes were considered differentially expressed if the *P*-value <0.0001. Genes of interest were clustered using Cluster software and viewed using TreeView. These microarray data were analyzed further using a nonparametric Mann–Whitney *U* test (Statistica, Tulsa, OK, USA) in order to identify genes that are statistically different between the C57BL/6.NOD-*Aec1Aec2* and C57BL/6 with a *P*-value <0.01.

Verification of Selected Genes by Semiquantitative RT-PCR

Total RNA was prepared from freshly explanted submandibular glands using the Rneazy Mini Kit (Qiagen, Valencia, CA, USA). cDNA was synthesized using 4 μg of total RNA, Superscript II reverse transcriptase (Invitrogen Life Technologies, Carlsbad, CA, USA), and pd(T)12–18 oligomeric DNA (Amersham Pharmacia, Piscataway, NJ, USA). The cDNA was quantified by spectrophotometry. Semiquantitative PCRs were carried out using 1 μg of cDNA as template. Following an initial denaturation at 94°C for 4 min, each PCR was carried out for 40 cycles consisting of 94°C for 1 min, optimal annealing temperature for 45 s and 72°C for 2 min. The forward and reverse sequences of each primer set are:

p38-forward:	5′-TCA ACC AGG AAG TGA GTG GCT GAA-3′
p38-reverse:	5′-ATC TTG GCA CCT CTC AGA GCC TTT-3′
Ch1-forward:	5′-AGC CAG ATC TGA AGC ACG TGA AGA-3′
Ch1-reverse:	5′-AGT GCTTCG TGA AGG GTC TCC AAT-3′
Adh5-forward:	5′-ATC TTG GGA CAT GAA GGT GCT GGA-3′
Adh5-reverse:	5′-ACG TTG CCA ATG CAC TCA AAG GAG-3′
B18-forward:	5′-GCA GCA GGG CAC CGT GAC AAA G-3′
B18-reverse:	5′-ACG CAG GAG GGC ATC AAA GAG CA-3′
Pfdn5-forward:	5′-GGC CCA CAT TTG GGT GGA AGA TTT-3′
Pfdn5-reverse:	5′-CGT TGCTCT TGT TCA GCA CGT TCA-3′
Stat-forward:	5′-TGGG GGA GGG GCC TTC TTG ATG-3′
Stat-reverse:	5′-TGG CCC CCT TAA TGG ATG TGC AA-3′
Pde4-forward:	5′-CCC GCG TCA GTG CCT TTG CTA T-3′
Pde4-reverse:	5′-CGG CGC TCC ATG AAG GTT CGT-3′
Rac1-forward:	5′-TGG GTG TGC TGG GTG GAG TGT GA-3′
Rac1-reverse:	5′-TGG GGA GGG ACG GCA GTG GAG-3′
Map2k4-forward:	5′-GCG ATG TGC TCA GCC AAA TTC CC-3′
Map2k4-reverse:	5′-CCT GGC CCA TGA TGT CGA GAA GC-3′
Jnk-forward:	5′-AGC TCG GAA CAC CTT GTC CTG AAT-3′
Jnk-reverse:	5′-AGC CAT TGA TCA TTG CTG CAC CTG-3′
Nfkb-forward:	5′-TTC TGC ATG GCG ATG TCA AAG CTG-3′
Nfkb-reverse:	5′-ATG CTG AGG CAG GAG AGG ATT TGT-3′
Traf6-forward:	5′-GCA CAA GTG CCC AGT TGA CAA TGA-3′
Traf6-reverse:	5′-AGT GTC GTG CCA AGT GAT TCC TCT-3′
BAFFR-2-forward:	5′-AGC AGT TCG GTT TGT GTG CTG TTC-3′
BAFFR-2-reverse:	5′-CCG CAG TGC ATT CTG GGA ATC AAA-3′
Baff-forward:	5′-AACGGAGACGACACCTTC TTTGGT-3′
Baff-reverse:	5′-CTGAACATGTGTCACCCA AGGCAA-3′
β-Actin-forward:	5′-CCT GAA CCC TAA GGC CAA CCG-3′
β-Actin-reverse:	5′-GCT CAT AGCTCT TCTCCA GGG-3′

PCR products were size separated by electrophoresis using a 0.9% agarose gels and visualized

with ethidium bromide staining. PCR band intensities were compared to β-actin using the Flourchem Imaging densitometer system (Alpha Innotech Corporation, San Leandro, CA, USA). Relative band intensities were determined by dividing the intensity of selected genes mRNA by the density of β-actin band.

Results

Differential Gene Expression in the Submandibular Glands of 8-week-old C57BL/6. NOD-*Aec1Aec2* Mice Normalized to 8-week-old C57BL/6J Mice

C57BL/6.NOD-*Aec1Aec2* mice exhibit both the pathophysiological characteristics and reduced secretory responses observed with NOD mice; however, the disease process appears to be accelerated in the C57BL/6.NOD-*Aec1Aec2* mouse suggesting either the genetic background of C57BL/6J contributes positively to the disease or the genetic background of NOD contributes some resistance genes.[2,23] The present study was designed to define gene expression profiles within the submandibular glands of C57BL/6.NOD-*Aec1Aec2* mice at two time points, 8 weeks of age (representing an early preclinical phase of disease) and 12 weeks of age (representing the early clinical phase of autoimmunity). By examining these two time points, genes identified as being differentially expressed may be correlated with one or more manifestations of abnormal glandular homeostasis and the initiation of the autoimmune response, thus enabling us to separate and dissect the pathophysiological *vs* immunological aspects of the SjS-like disease. The use of the C57BL/6J and C57BL/6.NOD-*Aec1Aec2* combination permits four comparisons: (1) C57BL/6J (8 weeks of age) *vs* C57BL/6J (12 weeks of age) showing normal age-related changes in gene expressions, (2) C57BL/6J (8 weeks of age) *vs* C57BL/6.NOD-*Aec1Aec2* (8 weeks of age) showing early phase disease-related gene expressions, (3) C57BL/6J (12 weeks of age) *vs* C57BL/6.NOD-*Aec1Aec2* (12 weeks of age) showing late phase disease-related gene expressions, and (4) C57BL/6J (8 weeks of age) *vs* C57BL/6.NOD-*Aec1Aec2* (12 weeks of age) showing changes in both age- and disease-initiating gene expressions. For the current study, the data from (2) and (4) are presented to focus on identification of possible underlying mechanisms for onset of SjS-like disease. We have utilized oligonucleotide microarrays, as opposed to cDNA arrays, making identification of differentially expressed genes faster, although recognizing that organ-specific genes may be missed.

A comparison of differentially expressed genes in the submandibular glands of C57BL/6.NOD-*Aec1Aec2 vs* C57BL/6J mice at 8 weeks of age (a time at which early preclinical manifestations should be evident and earliest infiltrations of leukocytes be present) identified 75 genes reaching statistical significance from the profiling of 10 752 genes. The expression profiles of these 75 genes are compared in Figure 1 between 5 individual samples from each strain, revealing the consistent differential

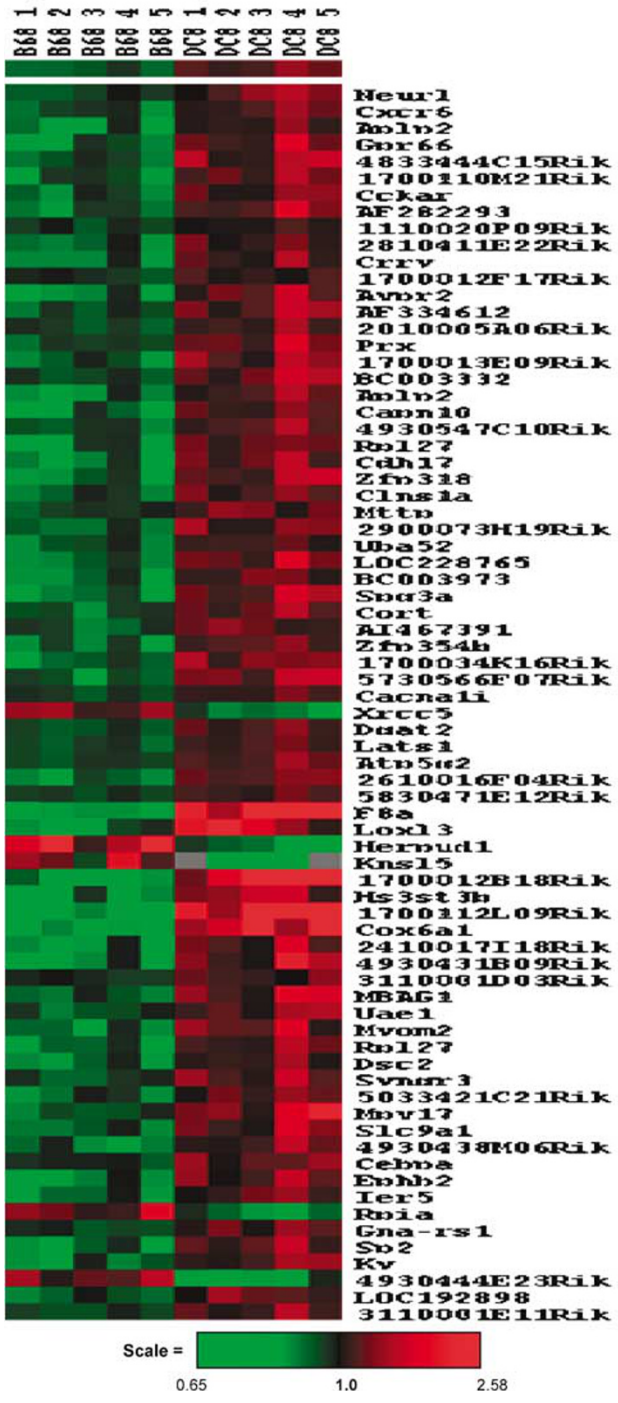

Figure 1 TreeView map of differentially expressed genes in the submandibular glands of 8-week-old C57BL/6.NOD-*Aec1Aec2* mice compared to those of 8-week-old C57BL/6 mice. cDNA from the submandibular glands of individual mice ($n = 5$ per group) were hybridized against a partial genomic oligonucleotide library (MWG Mouse 30 K A Arrays, MWG Biotech) and further analyzed for significant differences as determined by the Mann–Whitney *U* test (see Table 1). Upregulated genes are shown in red, while downregulated genes are shown in green.

expressions among the individual mice within each group. Of the 75 differentially expressed genes identified in this first analysis, 71 were upregulated and four downregulated in the C57BL/6.NOD-*Aec1Aec2* mice compared to the parental C57BL/6 mice. The mean expression levels for these 75 genes in the C57BL/6.NOD-*Aec1Aec2* mice normalized against the mean expression levels in the C57BL/6J mice are presented in Table 1 together with known biological functions. As might be expected, these genes are involved in multiple cellular functions, including DNA replication, transcription and translation, signal transduction and protein activation, as well as ion transport, metabolism and energy production. In addition, a number of genes encode membrane-associated proteins, while the functions of 15 genes remain unknown. Of particular interest is the fact that five genes are located on chromosome 1 (ie, *Ier5*, *Capn10*, *Xrcc5*, *Crry* and *Gpr66*) and two genes on chromosome 3 (ie, 4930431B09Rik and 4930444E23Rik).

Table 1 Relative differential gene expressions in submandibular glands from 8-week-old C57BL/6 mice *vs* 8-week-old C57BL/6.NOD-*Aec1Aec2* mice, as determined by the Mann–Whitney *U* test

Gene	*Gene description*	*B6:DC (8 weeks)*	P-*value*	*B6:DC (12 weeks)*	P-*value*
Signal transduction					
Cxcr6	Chemokine (C-X-C motif) receptor 6	1.25	<0.010	1.12	NS
Cckar	Cholecystokinin A receptor	1.29	<0.010	1.15	NS
Syngr3	Synaptogyrin 3	1.27	<0.010	1.39	<0.010
Myom2	Myomesin 2	1.39	<0.010	1.34	0.016
MBAG1	Leucine rich repeat containing 4	1.37	<0.010	1.20	NS
Neurl	Neuralized homolog (*Drosophila*)	1.26	<0.010	1.32	0.046
Avpr2	Arginine vasopressin receptor 2	1.41	<0.010	1.38	0.016
Prx	Periaxin	1.29	<0.010	1.61	<0.010
AF334612	PDZ domain containing 2	1.30	<0.010	1.36	<0.010
1700112L09Rik	Chimerin	2.16	<0.010	0.40	<0.010
LOC228765	Syndecan-binding protein (syntenin) 2	1.37	<0.010	1.28	NS
3110001E11Rik	RIKEN cDNA 3110001E11 gene	1.22	<0.010	1.26	<0.010
4930438M06Rik	RIKEN cDNA 4930438M06 gene	1.31	<0.010	1.24	NS
Transcription					
F8a	Factor 8-associated gene A	1.92	<0.010	0.36	<0.010
Zfp354b	Zinc-finger protein 354B	1.32	<0.010	1.39	<0.010
Zfp318	Zinc-finger protein 318	1.40	<0.010	1.22	NS
LOC192898	Zinc-finger CCCH type domain containing 5	1.25	<0.010	1.22	<0.010
BC003332	cDNA sequence BC003332	1.29	<0.010	1.14	NS
Sp2	Sp2 transcription factor	1.37	<0.010	1.24	0.047
2010005A06Rik	RIKEN cDNA 2010005A06 gene	1.22	<0.010	1.10	NS
4930547C10Rik	RIKEN cDNA 4930547C10 gene	1.26	<0.010	1.08	NS
2610016F04Rik	RIKEN cDNA 2610016F04 gene	1.36	<0.010	1.27	NS
Cell cycle					
5730566F07Rik	RIKEN cDNA 5730566F07 gene	1.38	<0.010	0.56	<0.010
Ier5	Immediate early response 5	1.29	<0.010	1.27	NS
Carbohydrate					
Rpia	Ribose 5-phosphate isomerase A	0.73	<0.010	0.74	<0.010
Lipid					
Uae1	Glucosamine	1.26	<0.010	1.50	<0.010
Protein					
Hs3st3b	Heparan sulfate (glucosamine) 3-O-sulfotransferase 3B	1.52	<0.010	0.61	<0.010
Herpud1	Homocysteine-inducible, endoplasmic reticulum stress-inducible, ubiquitin-like	0.60	<0.010	1.09	NS
Cort	Cortistatin	1.28	<0.010	1.17	NS
Rpl27	Ribosomal protein L27	1.35	<0.010	1.12	NS
Uba52	Ubiquitin A-52 residue ribosomal protein fusion product 1	1.24	<0.010	1.12	NS
2900073H19Rik	RIKEN cDNA 2900073H19 gene	1.30	<0.010	1.24	0.036
Gpr66	G protein-coupled receptor 66	1.37	<0.010	1.22	0.076
Cadherin associated					
AI467391	Casitas B-lineage lymphoma-like 1	1.25	<0.010	1.18	NS
Cdh17	Cadherin 17	1.41	<0.010	1.28	0.036
2010005A06Rik	RIKEN cDNA 2010005A06 gene	1.22	<0.010	1.38	<0.010

Table 1 Continued

Gene	*Gene description*	*B6:DC (8 weeks)*	P-*value*	*B6:DC (12 weeks)*	P-*value*
Immune system					
Crry	Complement receptor-related protein	1.32	<0.010	1.26	0.026
Energy production					
Atp5g2	ATP synthase, H+ transporting, mitochondrial	1.23	<0.010	1.19	NS
Knsl5	ATP-binding	0.41	<0.010	0.48	<0.010
BC003973	lysyl oxidase-like 1	1.31	<0.010	1.15	0.012
Protein kinase					
Lats1	Large tumor suppressor	1.21	<0.010	1.11	NS
Aplp2	Amyloid beta (A4) precursor-like protein 2	1.34	<0.010	1.26	NS
2810411E22Rik	RIKEN cDNA 2810411E22	1.26	<0.010	1.43	0.021
Ephb2	Eph receptor B2	1.38	<0.010	1.23	NS
Xrcc5	X-ray repair complementing defective repair in CH cells 5	0.72	<0.010	1.08	NS
Capn10	Calpain 10	1.38	<0.010	1.18	NS
Ky	Kyphoscoliosis	1.32	<0.010	1.12	NS
Cebpa	CCAAT/enhancer-binding protein (C/EBP), alpha	1.21	<0.010	0.99	NS
Ion channel/transport					
Clns1a	Chloride channel, nucleotide-sensitive, 1A	1.27	<0.010	1.30	NS
Slc9a1	Solute carrier family 9 (sodium/ hydrogen exchanger), member 1	1.33	<0.010	1.23	NS
Cacna1i	Calcium channel, alpha 1I subunit	1.18	<0.010	0.96	NS
2010005A06Rik	RIKEN cDNA 2010005A06 gene	1.22	<0.010	1.04	NS
Membrane protein					
Cox6a1	Cytochrome *c* oxidase, subunit VI a, polypeptide 1	1.83	<0.010	4.93	<0.010
Dgat2	Diacylglycerol *O*-acyltransferase 2	1.23	<0.010	1.26	0.027
Spg3a	Spastic paraplegia 3A homolog (human)	1.44	<0.010	1.52	<0.010
AF282293	Olfactory receptor 971	1.34	<0.010	1.27	0.044
Gna-rs1	Guanine nucleotide-binding protein, related sequence 1	1.21	<0.010	1.42	<0.010
Mpv17	Mpv17 transgene, kidney disease mutant	1.38	<0.010	1.39	<0.010
3110001D03Rik	RIKEN cDNA 3110001D03 gene	1.16	<0.010	1.10	<0.010
Dsc2	Desmocollin 2	1.28	<0.010	1.17	NS
Unknown function					
Loxl3	lysyl oxidase-like 3	1.62	<0.010	2.28	<0.010
1700013E09Rik	RIKEN cDNA 1700013E09 gene	1.34	<0.010	1.22	<0.010
2410017I18Rik	RIKEN cDNA 2410017I18 gene	1.41	<0.010	1.45	<0.010
AF282293	Olfr971-olfactory receptor 971	1.34	<0.010	1.27	0.044
5830471E12Rik	RIKEN cDNA 5830471E12 gene	1.19	<0.010	1.13	NS
1700034K16Rik	RIKEN cDNA 1700034K16 gene	1.36	<0.010	1.23	0.076
BC003332	cDNA sequence BC003332	1.29	<0.010	1.14	NS
1700013E09Rik	RIKEN cDNA 1700013E09 gene	1.34	<0.010	1.46	<0.010
4930444E23Rik	RIKEN cDNA 4930444E23 gene	0.65	<0.010	0.56	<0.010
1700012F17Rik	RIKEN cDNA 1700012F17 gene	1.14	<0.010	1.09	0.046
1110020P09Rik	RIKEN cDNA 1110020P09 gene	1.13	<0.010	1.10	NS
1700110M21Rik	RIKEN cDNA 1700110M21 gene	1.32	<0.010	1.22	0.012
4833444C15Rik	RIKEN cDNA 4833444C15 gene	1.34	<0.010	1.20	NS
5033421C21Rik	RIKEN cDNA 5033421C21 gene	1.28	<0.010	1.29	0.028
4930431B09Rik	RIKEN cDNA 4930431B09 gene	1.46	<0.010	1.35	0.028

A closer look at the genes that are differentially expressed at 8 week of age in the submandibular glands of C57BL/6.NOD.*Aec1Aec2* mice tend to link membrane proteins involved in signal transductions with intracellular trafficking, especially of vesicles. Genes that encode membrane proteins include *Dgat2*, *Spg3a*, *AF282293*, *Gna-rs1*, *Mpv17*, *1700042F02Rik*, *3110001D03Rik*, and *Dsc2*, and these, in turn, interact with various intracellular molecules, for example, G-proteins, Cckar, 1700112l09Rik, 2010005A06Rik, Gpr66, Gna-rs1 and Spg3a, which act as chaperones and affect the activity of other molecules. The ion channel molecules such as Cns1a, Slc9a1, AF334612 which are involved in the trafficking of the vesicles, apical sorting of the proteins and subsequent degradation are also upregulated. This is supported by the upregulation of CCKar, AF334612, Synaptogyrins and molecules like Ranbp2 and Cacna1i affecting exocrine secretion and calcium channels, respectively, potentially altering the vesicle transport and/ or saliva secretion. Additionally, calcium is known

to be important for the functions of cadherins. Removal of calcium reduces adhesive activity and renders cadherins vulnerable to proteases. As cadherins are critical to the maintenance of proper cell–cell contacts, they are important regulators of morphogenesis.[24] Two genes that regulate expression of cadherin molecules (Cdh17, AI467391 and Dsc2) were also found to be significantly upregulated.

Differential Gene Expression in the Submandibular Glands of 12-week-old C57BL/6.NOD-*Aec1Aec2* Mice Normalized to 8-week-old C57BL/6J Mice

A comparison of differentially expressed genes in the submandibular glands of C57BL/6.NOD-*Aec1Aec2* at 12 weeks of age (a time of detectable clinical manifestations characterized by small areas of leukocyte infiltrates) *vs* C57BL/6J mice at 8 weeks identified 105 genes that reached statistical significance in the profiling of the same 10 752 genes analyzed above. The expression profile of these 105 differentially expressed genes is presented in Figure 2, again revealing a consistent differential expression among the individual mice within each group. Of the 105 genes, 85 were upregulated and 20 downregulated. A listing of the known biological functions of these 105 genes is presented in Table 2. These genes encode molecules involved in DNA replication, transcription and translation, protein folding and transport, signal transduction and protein activation, as well as ion transport, metabolism and energy production. In addition, a number of genes encode membrane-associated proteins and proteins involved in intracellular trafficking, ribosomal biogenesis, free-radical neutralization, and immune regulation. The functions of some 25 genes remain unknown. Of the differentially expressed genes, five are located on chromosome 1 (ie, *Stx6*, *Rpl37a*, *Cdh74921511D23Rik*, *1190006A08Rik* and *1500032H18Rik*) and four on chromosome 3 (ie, *H2afz*, *Adh5*, *6330415M09Rik* and *4930415G15Rik*).

As might be expected from the known pathophysiological analyses of C57BL/6.NOD-*Aec1Aec2* mice, several of the genes which were significantly upregulated are associated with either programmed cell death or immune functions. Genes *Ppard*, *Gabrr2*, *Gabrb2*, *Pde4b*, *F2rl1*, *B2m*, *Mtcp*, *Cd5*, *2410003B16Rik*, *2310043N20Rik*, *Jcam2*, *Fut8* and *Nfkbib* certainly can affect cellular homeostasis through various chemokines, TNF-α responses or MAP kinases eventually leading to apoptosis of the cells. Another group of overexpressed genes includes *Synaptogyrins*, *Synt6 Gabrb2*, *Cdh7*, *1700012B18Rik*, *Atp8a1* and *Aqp2* each associated with intracellular trafficking and vesicular transport through ion channels. These genes can regulate the movement of vesicles from the basal lateral to the apical membrane and possibly contribute to the flow

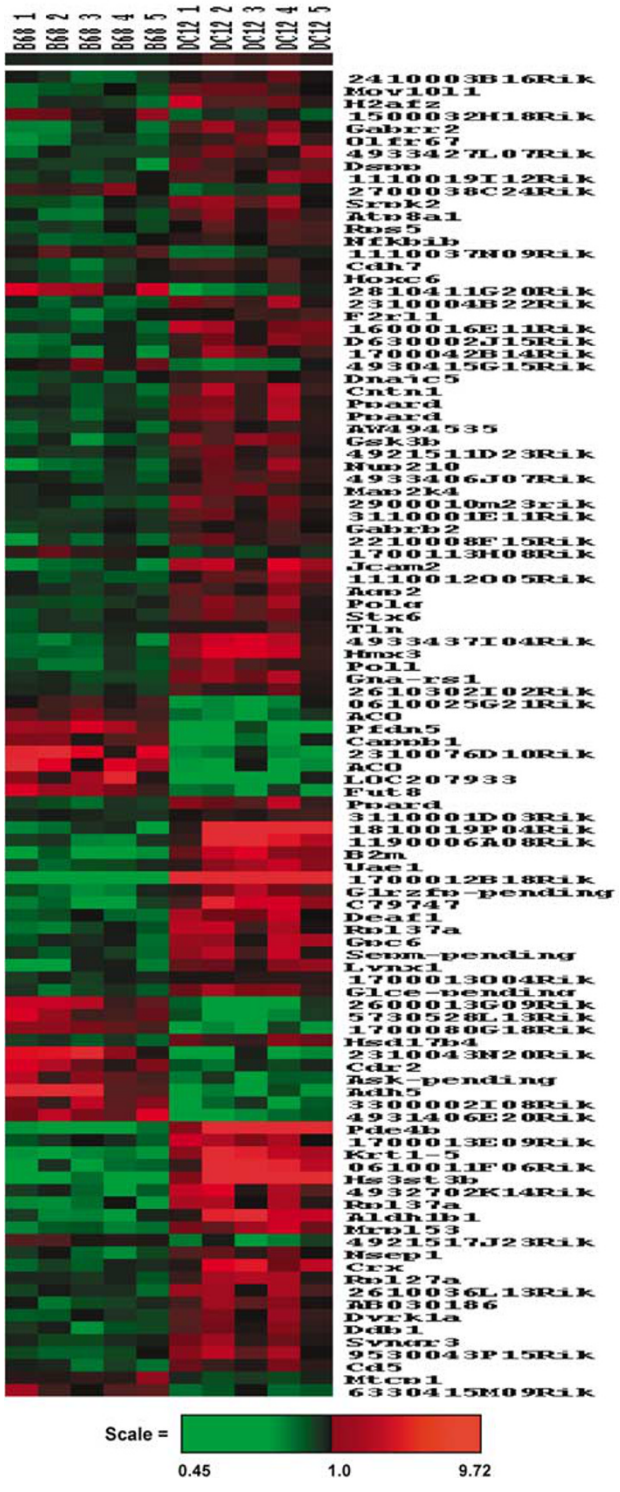

Figure 2 TreeView map of differentially expressed genes in the submandibular glands of 12-week-old C57BL/6.NOD-*Aec1Aec2* mice compared to those of 8-week-old C57BL/6 mice. cDNA from the submandibular glands of individual mice ($n=5$ per group) were hybridized against a partial genomic oligonucleotide library and further analyzed as in Figure 1. Upregulated genes are shown in red, while downregulated genes are shown in green.

rates of saliva. Interestingly, a similar comparison for differentially expressed genes in the submandibular glands of 12-week-old *vs* 8-week-old C57BL/6J

Table 2 Relative differential gene expressions in submandibular glands from 8-week-old C57BL/6 mice *vs* 12-week-old C57BL/6.NOD-*Aec1Aec2* mice, as determined by the Mann–Whitney *U* test

Gene	*Gene description*	*B6:DC (12 weeks)*	P-*value*	*B6:DC (8 weeks)*	P-*value*
Signal transduction					
Ppard	Peroxisome proliferator activator receptor delta	1.45	<0.010	1.16	<0.010
Gabrr2	Gamma-aminobutyric acid (GABA-C) receptor, subunit rho-2	1.42	<0.010	1.31	0.012
Gabrb2	Gamma-aminobutyric acid (GABA-A) receptor, beta 2	1.17	<0.010	1.06	0.046
Pde4b	Phosphodiesterase 4B, cAMP specific	4.27	<0.010	1.51	<0.010
F2rl1	Coagulation factor II (thrombin) receptor-like 1	1.30	<0.010	0.99	NS
4921511D23Rik	RIKEN cDNA 4921511D23 gene	1.26	<0.010	1.10	NS
Cntn1	Contactin 1	1.45	<0.010	1.18	NS
Transcrpition					
Nsep1	Nuclease sensitive element binding protein 1	1.35	<0.010	1.01	NS
Crx	Cone-rod homeobox containing gene	1.56	<0.010	1.06	NS
Deaf1	Deformed epidermal autoregulatory factor 1 (*Drosophila*)	1.48	<0.010	1.27	0.021
Ddb1	Damage specific DNA binding protein 1	1.38	<0.010	1.08	NS
Mov10l1	Moloney leukemia virus 10-like 1	1.30	<0.010	1.19	0.028
H2afz	H2A histone family, member Z	1.40	<0.010	1.21	0.012
Hoxc6	Homeobox C6	1.23	<0.010	1.02	NS
Polg	Polymerase (DNA directed), gamma	1.36	<0.010	1.16	0.012
2810411G20Rik	RIKEN cDNA 3010019O03 gene	0.60	<0.010	0.63	0.016
9530043P15Rik	Ribonuclease A family, member 6	1.45	<0.010	1.24	NS
Cdr2	Cerebellar degeneration-related 2	0.70	<0.010	0.94	NS
Hmx3	H6 homeobox 3	1.67	<0.010	1.16	NS
Nfkbib	Nuclear factor, kappa light chain gene enhancer inhibitor, beta	1.28	<0.010	1.16	0.036
Intracellular trafficking					
Syngr3	Synaptogyrin 3	1.32	<0.010	1.28	<0.010
Nup210	Nucleoporin 210	1.41	<0.010	1.30	<0.010
Stx6	Syntaxin 6	1.30	<0.010	1.11	NS
Poll	Polymerase (DNA directed), lambda	1.43	<0.010	1.12	NS
2700038C24Rik	Exportin 5	0.77	<0.010	0.97	NS
Cytoskeletal proteins					
Krt1-5	Keratin complex 1, acidic, gene 5	2.25	<0.010	1.29	0.021
Tln	Talin	1.19	<0.010	1.12	<0.010
Cappb1	Capping protein (actin filament) muscle Z-line, beta	0.62	<0.010	0.71	0.016
GTPase-associated					
Gna-rs1	Guanine nucleotide-binding protein,	1.43	<0.010	1.21	<0.010
2600013G09Rik	RAB, member of RAS oncogene family-like 4	0.50	<0.010	0.86	NS
Protein					
Pfdn5	Prefoldin 5/protein folding	0.45	<0.010	0.62	NS
G1rzfp-pending	Ring finger protein 130	1.54	<0.010	1.03	NS
1600016E11Rik	Prolactin-like protein I/hormone activity	1.47	<0.010	1.19	NS
2310004B22Rik	RIKEN cDNA 4930404J24 gene	1.42	<0.010	1.33	0.015
Dnajc5	Hsp40 homolog, subfamily C, member 5 molecular chaperone	1.23	<0.010	1.09	NS
4933406J07Rik	RIKEN cDNA 4933406J07 gene/KRAB protein	1.30	<0.010	1.02	NS
3300002I08Rik	RIKEN cDNA 3300002I08 gene/KRAB protein	0.62	<0.010	0.93	NS
AW494535	F-box only protein 4	1.27	0.000	1.28	0.004
2610302I02Rik	Purinergic receptor (family A group 5) G-protein	1.23	<0.010	1.11	NS
Olfr67	Olfactory receptor 67/G-protein coupled receptor protein	1.39	<0.010	1.25	0.036
1110019I12Rik	Selenoprotein N, 1 unknown fn	1.31	<0.010	1.17	NS
Sepm	Selenoprotein M	1.49	<0.010	1.31	0.028
Ribosomal proteins					
Rpl37a	Ribosomal protein L37a	1.50	<0.010	1.37	0.016
Rpl27a	Ribosomal protein L27a	1.41	<0.010	1.18	0.047
Mrpl53	Mitochondrial ribosomal protein L53	1.62	<0.010	1.22	<0.010
Rps5	Ribosomal protein S5	1.24	<0.010	1.17	0.021
Electron transport					
2310076D10Rik	24-Dehydrocholesterol reductase	0.51	<0.010	1.38	NS
Aldh1b1	Aldehyde dehydrogenase 1 family, member B1	1.97	<0.010	1.19	NS
Adh5	Alcohol dehydrogenase 5 (class III), chi polypeptide	0.49	<0.010	0.66	NS

Table 2 Continued

Gene	*Gene description*	*B6:DC (12 weeks)*	P-*value*	*B6:DC (8 weeks)*	P-*value*
Proteinkinase					
Gsk3b	Glycogen synthase kinase 3 beta	1.43	<0.010	1.08	NS
Dyrk1a	Dual-specificity tyrosine-(Y)-phosphorylation regulated kinase 1a	1.31	<0.010	1.24	<0.010
Ask-pending	Expressed sequence AA545217	0.66	<0.010	0.96	NS
Map2k4	Mitogen activated protein kinase kinase 4	1.23	<0.010	1.18	0.012
Srpk2	Serine/arginine-rich protein specific kinase 2	1.39	<0.010	1.17	NS
ACO	Human-kallikrein 15	0.52	<0.010	1.01	NS
0610025G21Rik	RIKEN cDNA 0610025G21 gene	0.68	<0.010	0.89	NS
6330415M09Rik	RIKEN cDNA 63300415M09 gene	0.75	<0.010	0.86	NS
Membrane protein					
Fut8	Fucosyltransferase 8	0.61	<0.010	0.94	NS
B2m	Beta-2 microglobulin	1.97	<0.010	1.06	NS
Hs3st3b	Heparan sulfate (glucosamine) 3-O-sulfotransferase 3B	3.14	<0.010	1.48	<0.010
Jcam2	Junction adhesion molecule 2	1.67	<0.010	1.42	0.016
Gpc6	Glypican 6	1.44	<0.010	1.31	0.036
1700013O04Rik	Chemokine-like factor super family 2B	1.15	<0.010	1.03	NS
3110001D03Rik	RIKEN cDNA 3110001D03 gene	1.18	<0.010	1.16	<0.010
Immunity					
Mtcp1	Mature T-cell proliferation 1	0.79	<0.010	1.05	NS
Cd5	CD5 antigen	1.36	<0.010	1.19	0.028
2410003B16Rik	RIKEN cDNA 2410003B16 gene	1.30	<0.010	1.10	NS
2310043N20Rik	Interleukin 1 family, member 8	0.44	<0.010	0.58	0.028
Neurotoxin activity					
Lynx1	Ly6/neurotoxin 1/Chrnb2 cholinergic receptor, nicotinic, beta polypeptide 2	1.45	<0.010	1.41	<0.010
Lipid metabolism					
Hsd17b4	Hydroxysteroid (17-beta) dehydrogenase 4	1.38	<0.010	1.17	NS
Carbohydrate metabolism					
Glce	Glucuronyl C5-epimerase	1.47	<0.010	1.28	<0.010
Uae1	Glucosamine	1.51	<0.010	1.27	<0.010
Extracellular matrix					
Dspp	Dentin sialophosphoprotein	1.35	<0.010	1.11	NS
Inhibits the growth of E. coli					
AB030186	RIKEN cDNA B230317C12 gene	1.40	<0.010	1.25	0.016
Ion channel					
Cdh7	Cadherin 7, type 2	1.29	<0.010	1.17	0.047
Atp8a1	ATPase, aminophospholipid transporter (APLT), class I, type 8A, member 1	1.41	<0.010	1.06	NS
Aqp2	Aquaporin 2	1.28	<0.010	1.15	NS
Function not known					
1700080G18Rik	RIKEN cDNA 1700080G18 gene	0.58	<0.010	0.77	<0.010
4931406E20Rik	RIKEN cDNA 4931406E20 gene	0.54	<0.010	0.63	<0.010
4933437I04Rik	RIKEN cDNA 4933437I04 gene	1.70	<0.010	1.30	<0.010
1110012O05Rik	RIKEN cDNA 1110012O05 gene	1.42	<0.010	0.96	NS
1700113H08Rik	RIKEN cDNA 1700113H08 gene	0.81	<0.010	0.88	NS
2210008F15Rik	Nucleolar protein 7	1.34	<0.010	1.04	NS
2900010m23rik	RIKEN cDNA 2900010M23 gene	1.36	<0.010	1.15	NS
4930415G15Rik	RIKEN cDNA 4930415G15 gene	0.70	<0.010	0.94	NS
1700042B14Rik	RIKEN cDNA 1700042B14 gene	1.44	<0.010	1.08	NS
D630002J15Rik	RIKEN cDNA D630002J15 gene	1.34	<0.010	1.24	<0.010
1190006A08Rik	RIKEN cDNA 1190006A08 gene	1.94	<0.010	1.20	0.047
1110037N09Rik	RIKEN cDNA 1110037N09 gene	0.76	<0.010	0.88	0.016
4933427L07Rik	RIKEN cDNA 4933427L07 gene	1.33	<0.010	1.07	NS
1500032H18Rik	RIKEN cDNA 1500032H18 gene	0.76	<0.010	1.07	NS
5730528L13Rik	RIKEN cDNA 5730528L13 gene	0.61	<0.010	1.00	NS
1810019P04Rik	RIKEN cDNA 1810019P04 gene	2.71	<0.010	1.50	0.028
2610036L13Rik	RIKEN cDNA 2610036L13 gene	1.39	<0.010	1.19	0.016
LOC207933	Isopentenyl-diphosphate delta-isomerase-like	0.52	<0.010	0.72	NS
4932702K14Rik	RIKEN cDNA 4932702K14 gene	1.63	<0.010	1.59	NS

Table 2 Continued

Gene	*Gene description*	*B6:DC (12 weeks)*	P-*value*	*B6:DC (8 weeks)*	P-*value*
0610011F06Rik	RIKEN cDNA 0610011F06 gene	2.21	<0.010	1.23	0.028
1700013E09Rik	RIKEN cDNA 1700013E09 gene	1.44	<0.010	1.32	<0.010
4921517J23Rik	RIKEN cDNA 4921517J23 gene	0.75	<0.010	1.01	NS
3110001E11Rik	Unknown fn	1.26	<0.010	1.22	<0.010
C79747	Unknown (protein for image:3491533)	1.92	<0.010	1.13	NS
1700012B18Rik	Pregnancy-induced growth inhibitor	10.15	<0.010	2.70	NS

Table 3 Verification of selected genes by semiquantitative RT-PCR

	8 weeks	*MA-8 weeks*	*SQ-8 weeks*	*12 weeks*	*MA-12 weeks*	*SQ-12 weeks*
1	*1700012B18Rik*	2.70[a]	2.31	*B18Rik*	10.15	2.52
2	*Traf6*	2.67	1.78	*Pde4b*	4.27	2.18
3	*1700112L09Rik*	2.16	1.91	*BaffR*	1.30	1.41
4	*Pde4b*	1.51	1.41	*Stat1*	1.33	1.48
5	*Stat1*	1.20	1.16	*Map2k4*	1.18	1.22
6	*Map2k4*	1.18	1.09	*Rac 1*	1.18	1.18
7	*Baff*	1.10	1.11	*p38beta*	1.07	1.35
8	*Rac 1*	1.06	1.06	*Baff*	0.97	0.96
9	*BaffR*	0.96	1.06	*Traf6*	0.95	0.96
10	*Jnk*	0.93	1.07	*Jnk*	1.05	1.05
11	*p38beta*	0.82	0.77	*Nfkb*	1.04	1.04
12	*Adh5*	0.66	0.78	*Pfdn5*	0.45	0.64
13	*Pfdn5*	0.62	0.71	*Adh5*	0.49	0.55
14	*Nfkb*	0.59	0.79	*1700112L09Rik*	0.40	0.46

[a]All values are normalized to gene expressions measured in submandibular glands of C57BL/6 mice at 8 weeks.

mice revealed 90 genes that reached statistical significance. (These data can be found in Supplemental Figure 1 and Supplemental Table 1.) Many of these genes appear to be involved in neural or epithelial cell development, as well as cellular homeostasis. All proved to be distinct from the genes differentially expressed in 12-week-old C57BL/6.NOD-*Aec1Aec2* submandibular glands.

Validation of Microarray Data by SemiQuantitative RT-PCR

To verify the overall results obtained from the microarrays, a number of genes were selected randomly for semiquantitative RT-PCR analysis. Genes were selected that were expressed at higher levels, lower levels and equal levels between the C57BL/6.NOD-*Aec1Aec2* and C57BL/6 mice, as determined by microarray analyses. As shown in Table 3, the relative expression of these genes in the submandibular glands, as determined by RT-PCR, proved highly consistent with the relative expressions obtained from the microarrays. Furthermore, the calculated differential expressions proved to be greater by microarray than by RT-PCR, consistent with published data (Eckenrode *et al*[25] and personal observations).

Association between Selected Differentially-Expressed Genes and SjS-like Autoimmune Exocrinopathy

Identification of large numbers of individual genes that are differentially expressed temporally can present a daunting task in data interpretation. However, this task can be simplified if several functionally associated genes can be linked. One interesting example of functionally linked genes identified by microarray involves cellular apoptosis. As reported in our earlier studies,[4,7,9,26] a wave of apoptosis occurs in the early phases of SjS-like disease, during which time there is a concomitant increased expression of caspase 3. As presented in Table 4, the *caspase 3* gene was found to be highly upregulated at 8 weeks of age in the submandibular glands of C57BL/6.NOD-*Aec1Aec2* mice, when analyzed by the Student's *t* test. Unexpectedly, however, a second caspase gene, *caspase 11*, was also significantly upregulated, while other caspase genes and mitochondria-associated apoptotic genes were not. As caspase-11 is generally induced by proinflammatory stimuli (Schauvliege *et al*[27] especially IL-1 and tumor necrosis factor (TNF)-associated proteins, genes of the TNF superfamily represented on the array were selected and examined. As listed in Table 5 in the order of differential expression observed at 8 weeks of age, only about

Table 4 Expression of apoptosis-related genes

Gene	*Full name*	*8 weeks*	P-*values (8 weeks)*[a]	*12 weeks*	P-*values (12 weeks)*[a]
Casp2	Caspase 2	1.25	0.02	1.19	0.14
Casp3	Caspase 3	2.17	0.47	0.92	0.68
Casp8ap2	Caspase 8-associated protein 2	0.81	0.05	0.97	0.80
Cflar	Casp8 and fadd-like apoptosis regulator	0.94	0.47	0.94	0.28
Casp9	Caspase 9	0.71	0.03	0.67	0.01
Casp11	Caspase 11	2.60	0.39	0.95	0.69
Casp12	Caspase 12	0.90	0.23	1.09	0.22
Casp14	Caspase 14	0.89	0.39	0.88	0.01
Bad	Bcl2-associated death promoter	0.91	0.62	1.13	0.30
Bak1	Bcl2 antagonist/killer	0.61	0.03	0.53	0.04
Bax	Bcl2-associated X protein	0.92	0.64	0.83	0.15
bag1	Bcl2-associated athanogene 1	1.06	0.67	1.19	0.27
daxx	Fas death domain-associated protein	0.86	0.29	1.19	0.28

[a]*P*-values determined by the Student's *t* test.

Table 5 Differentially expressed tumor necrosis factor (TNF) super family genes at 8 and 12 weeks of age as determined by microarray analyses

Gene	*Name of gene*	*8 weeks*[a]	P-*values (8 weeks)*[a]	*12 weeks*	P-*values (12 weeks)*[a]
traf6	TNF receptor-associated factor 6	2.67	0.06	0.95	0.180
tnfip6	TNF-induced protein 6	2.65	0.04	0.97	0.204
tnfaip1	TNF-induced protein 1	2.10	0.06	0.69	0.16
tnfrsf13b	TNF-receptor superfamily, member 13b	1.83	0.5	1.17	0.5
tnfsf7	TNF (ligand) superfamily, member 7	1.38	0.056	1.11	0.04
traf1	TNF-receptor-associated factor 1	1.31	0.26	1.09	0.834
litaf	Lps-induced TNF-alpha factor	1.25	0.6	0.92	0.013
tnfsf9	TNF (ligand) superfamily, member 9	1.22	0.14	0.97	0.466
tnfaip3	TNF-induced protein 3	1.13	0.42	1.35	0.04
tnfsf13b	TNF (ligand) superfamily, member 13b	1.10	0.103	0.97	0.51
tnfsf13	TNF (ligand) superfamily, member 13	1.10	0.916	0.97	0.34
tnfsf8	TNF (ligand) superfamily, member 8	1.07	0.012	0.69	0.06
tnfrsf19	TNF-receptor superfamily, member 19	1.01	0.013	1.26	0.05
tnfrsf8	TNF-receptor superfamily, member 8	0.98	0.446	1.03	0.09
tnfsf14	TNF (ligand) superfamily, member 14	0.98	0.287	1.19	0.06
tnfsf4	Tax-transcriptionally activated glycoprotein 1 ligand	0.97	0.116	0.85	0.980
tnfrsf13c	Baff receptor	0.96	0.013	1.30	0.06
ripk1	Receptor (tnfrsf)-interacting serine-threonine kinase 1	0.92	0.06	0.92	0.790
tnfrsf21	TNF-receptor superfamily, member 21	0.92	0.072	1.07	0.743
tnfrsf23	Tumor necrosis factor receptor superfamily, member 23	0.90	0.879	0.95	0.05
tnfrsf12	TNF-receptor superfamily, member 12	0.85	0.023	1.06	0.096
traf3	TNF receptor-associated factor 3	0.84	0.04	1.25	0.0425
tnfrsf5	TNF-receptor superfamily, member 5	0.82	0.105	1.04	0.214
tnfrsf11a	TNF-receptor superfamily, member 11a	0.81	0.88	0.84	0.126
tnfaip2	TNF-induced protein 2	0.81	0.089	0.86	0.0421
traf4	TNF-receptor associated factor 4	0.80	0.065	0.75	0.056
tnfrsf4	Tax-transcriptionally activated glycoprotein 1	0.79	0.045	0.92	0.013
tnfrsf17	TNF-receptor superfamily, member 17	0.78	0.068	1.11	0.011
tnfsf10	TNF-related apoptosis inducing ligand	0.73	0.06	0.72	0.033

[a]Expression of TNF genes in submandibular glands of C57BL/6J.NOD-*Aec1Aec2* mice are listed in order of expression at 8 weeks of age normalized against 8-week-old C57BL/6J mice.

six of the nearly 30 TNF genes, that is, *traf6, tnfip6, tnfaip1, tnfrsf13b, tnfsf7* and *traf1*, were upregulated when compared to those in sex- and age-matched C57BL/6 mice. While most of these genes showed a relative loss of upregulated expression by 12 weeks of age, *tnfaip3* (TNF-alpha inducible protein-1), *traf3, tnfrsf19* (TAJ/TROY), *tnfrsf13* (BAFF receptor) and possibly *tnfsf14* (LIGHT) were temporally upregulated in the submandibular glands at 12 weeks as compared to 8 weeks of age. Thus, these results are consistent with immunohistochemical data indicating that a wave of apoptosis occurs around 8 weeks of age in the submandibular glands of C57BL/6.NOD-*Aec1Aec2* or NOD mice[26,28] and, at the same time, provides evidence of a possible novel pathway involving caspase-11 underlying acinar cell apoptosis. Similarly, an upregulation of TAJ/TROY, BAFF-receptor and LIGHT at 12 weeks

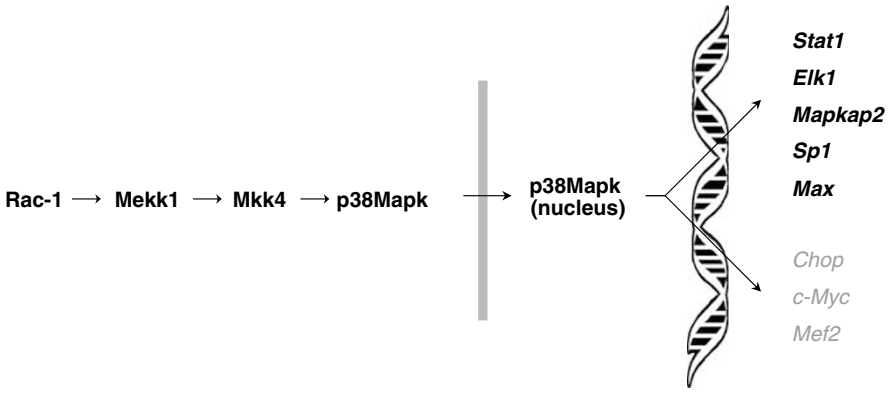

Figure 3 Differential regulation of genes in the submandibular glands of C57BL/6.NOD-*Aec1Aec2* mice between 8 and 12 weeks of age controlled through the Rac-1 signal transduction pathway. Genes upregulated are indicated in bold, while those downregulated are indicated in grey. Genes within this set but not on the microarray include *Atf2, Msk1, Creb, Histone H3* and *Hmg14*.

suggests an appearance of neuro-immunological processes, known to begin around this time.

A second set of functionally associated genes involving the Rac1/MEKK1 signal transduction pathway was examined based on the strong change in the relative gene expression levels exhibited by *chimerin* (Rac1 suppressor) between 8 weeks and 12 weeks of age (ie, a 2.16-fold increase *vs* a 2.5-fold decrease, respectively) (see Table 2). The Rac1/PI3 K and Rac1/MEKK1 signal transduction pathways are involved in cell proliferation, survival and programmed cell death involving the PKA, ERK1/2, SAPK/JNK and p38-MAPK downstream pathways. Genes within these various pathways present on the array were found to be upregulated significantly in the submandibular glands at 12 weeks of age compared to 8 weeks of age (Figure 3), as determined by the Student's *t* test, and these differential expressions were confirmed by RT-PCR profiling. When analyzed more closely, other genes, especially nuclear-associated genes such as *c-jun, elk1, sp1, max, Mapkap2* and *stat1*, were upregulated, while the genes *chop, met2* and *c-myc* were found to be downregulated. Interestingly, the upregulation of *NF-kB* was coordinated with the upregulated expression of *mekk1*. Thus, these microarray data point to major temporal changes in gene expression patterns indicative of major alterations in the homeostasis of the submandibular glands between 8 and 12 weeks of age.

Discussion

With the present study, we have applied microarray technology to identify genes that are differentially regulated during early development and onset of SjS-like disease associated with the NOD mouse model. To reduce background noise, we have taken advantage of our recently constructed C57BL/6.NOD-*Aec1Aec2* mouse strain, a C57BL/6J mouse containing two genetic regions derived from the NOD mouse capable of conferring full-blown SjS-like disease in the resulting congenic mice.[23] This permits a direct comparison between disease-prone C57BL/6.NOD-*Aec1Aec2* mice and their parental C57BL/6 partners that exhibit no evidence of SjS-like disease at the time points evaluated. Previous investigations of C57BL/6.NOD-*Aec1Aec2* mice have shown that the *Aec2* region on chromosome 1 regulates the numerous pre-disease pathophysiological changes in the salivary and lacrimal glands, while the *Aec1* region on chromosome 3 controls the autoimmune response leading to clinical disease.[2,23] Thus, this C57BL/6J–C57BL/6.NOD-*Aec1Aec2* congenic mouse combination represents an excellent model for identifying candidate genes responsible for both the early development and eventual onset of SjS-like disease.

To identify candidate genes possibly involved in the early phases of autoimmune xerostomia, we carried out microarray analyses using cDNA prepared from submandibular glands of C57BL/6.NOD-*Aec1Aec2* and C57BL/6 mice at two ages: 8 weeks, when the mice exhibit an early preclinical disease, and 12 weeks, when the mice exhibit the first overt signs of an impending autoimmune disease. Histological examinations of the submandibular glands show increased acinar cell apoptosis[13,28] at the 8 week time point, and first signs of leukocytic infiltration at the 12 week time point,[2,23] although the presence of small numbers of leukocytes (especially dendritic cells and macrophages) are no doubt present in the submandibular glands at both time points. Our comparison of gene expressions between C57BL/6J and C57BL/6.NOD-*Aec1Aec2* mice identified some 75 genes at 8 weeks and 105 genes at 12 weeks of age that were differentially expressed ($P<0.01$) based on the Mann–Whitney *U* test, with additional genes being identified using less stringent criteria with the Student's *t* test. While genes differentially expressed at 8 weeks of age in the C57BL/6.NOD-*Aec1Aec2* mouse encode products primarily involved in normal cellular processes like transcription, translation, DNA replication, signal transduction, vesicle trafficking and

metabolism, the genes differentially expressed at 12 weeks of age encode additional products involved in oxidative phosphorylation, free-radical neutralization, ion channel activity, protein processing and immune function. Using semi-quantitative RT-PCR, we were able to validate the relative levels of gene expressions observed with microarrays. Overall, these data indicate major changes in cellular homeostasis occur in the submandibular glands of C57BL/6.NOD-*Aec1Aec2* mice during this critical 4 week time frame.

Based on genes differentially expressed at a statistically significant level, together with genes that are known to cluster with the identified genes, a number of signal transduction pathways could be identified that apparently are temporally activated and potentially important to onset of SjS-like disease. Several of these pathways are depicted in Figures 4 and 5, and discussed in detail below. Genes differentially expressed in the submandibular glands of C57BL/6.NOD-*Aec1Aec2* mice at 8 weeks of age compared to those of age- and sex-matched C57BL/6J mice include several genes encoding molecules associated with apoptosis, for example, *F8a*, *Aplp2*, *Capn10*, *Cebpa* and *Xrcc5* (*Ku80*). In addition, two cysteine protease genes known to enhance apoptosis, specifically those encoding for caspase-3 and caspase-11, are both upregulated at 8 weeks. While caspase-11 is not expressed constitutively in most cell types, its expression is rapidly induced by proinflammatory stimuli such as LPS or IFN-γ as a result of NF-kB and/or STAT1 binding to its promoter.[27] While activation of caspase-11 can lead to caspase-3 activation, it can also promote caspase-1 activation and subsequent production of IL-1β and/or IL-18.[29] Based on the fact that *NF-kB* is not notably upregulated until 12 weeks of age together with our earlier observation in the NOD mouse that expression of IFN-γ in the submandibular gland is increased in very young mice,[30] we would propose that caspase-11 expression at 8 weeks of age is through STAT1 rather than NF-kB (see Figure 4).

This upregulation of the *caspase-11* and *caspase-3* genes rather than *caspase-9* and *bax*, together with alterations in specific TNF/TNFR family gene expressions (especially *traf6* and *traf1*) and the early presence of IFN-γ, all support the hypothesis that an increase in proinflammatory cytokines (possibly from pattern recognition of extrinsic bacterial/viral

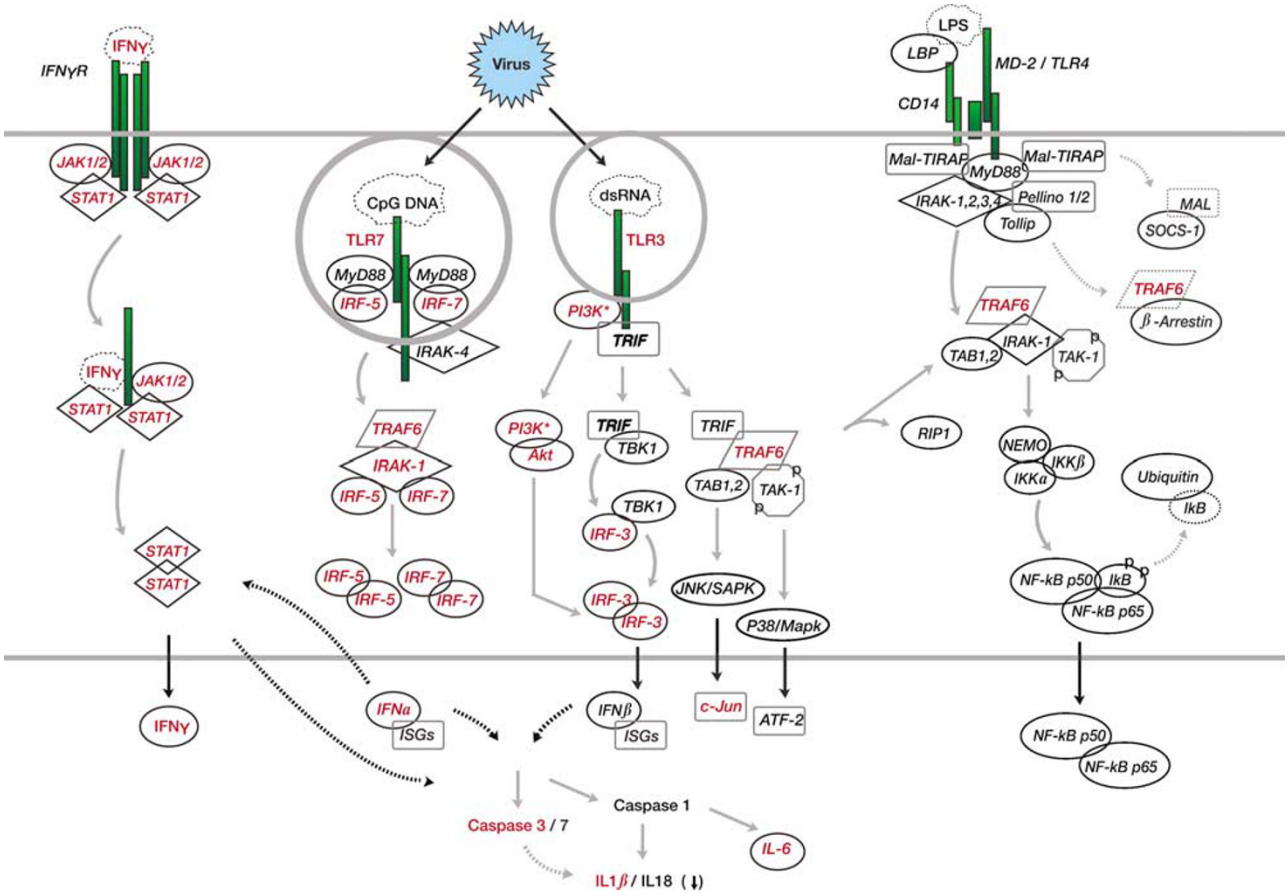

Figure 4 Summary of upregulated genes and signal transduction pathways in submandibular glands of C57BL/6.NOD-*Aec1Aec2* mice at 8 weeks of age. Genes found to be upregulated are shown in red, while genes found to be downregulated or not represented on the microarrays are shown in black. Discussion of these genes and pathways is presented in the text.

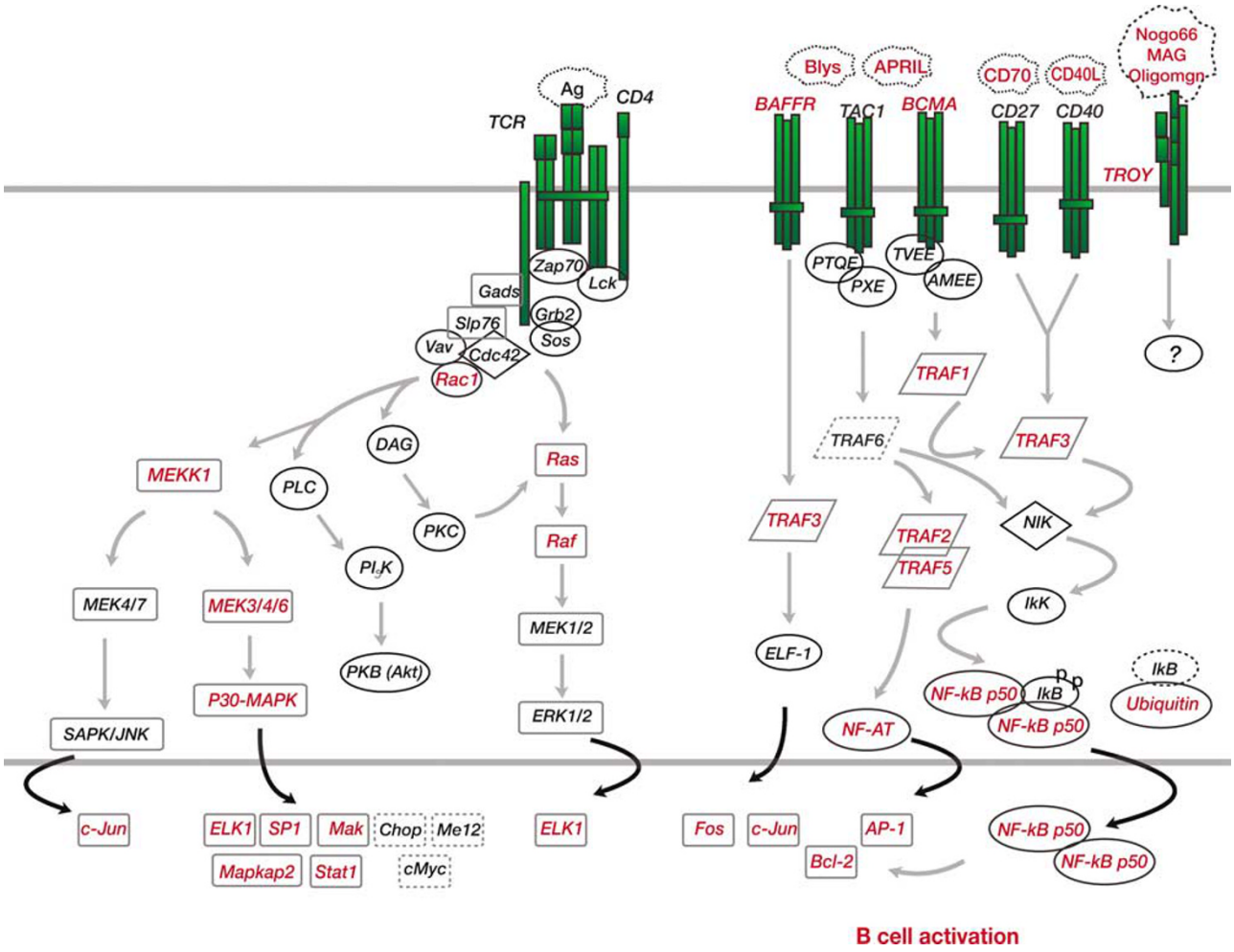

Figure 5 Summary of upregulated genes and signal transduction pathways in submandibular glands of C57BL/6.NOD-*Aec1Aec2* mice at 12 weeks of age. Genes found to be upregulated are shown in red, while genes found to be downregulated or not represented on the microarrays are shown in black. Discussion of these genes and pathways is presented in the text.

pathogen stimuli through toll-like receptor (TLR) signal transduction pathways) leads to the activation of cell death-mediated or ER-mediated rather than mitochondria-mediated pathways. Consistent with this concept is the known increased expressions of ICE, NEDD-2 and Apopain/CCP in NOD mice.[28] Interestingly, the TLR pathways whose genes were identified as being upregulated involves *Irf3, Irf5* and *Irf7* signaling, all endosome-associated TLRs (Figure 4). Genes associated with TLR pathways whose recognition patterns generally involve bacteria (TLR4, TLR1, TLR2 and TLR6) remained unchanged. Nevertheless, it remains premature to conclude that specific cell death-mediated and/or ER-mediated pathways are responsible for the enhanced apoptosis in the exocrine glands of C57BL/6.NOD-*Aec1Aec2* mice prior to disease onset without first examining more closely, by other experimental approaches, molecules that are involved in mitochondria-mediated pathways, for example, cytochrome *c*, Apaf-1, Bax and caspase-9. In any event, since apoptosis and other intrinsic alterations appear to play a major role in the early stages of SjS-like disease in the mouse model, and possibly in humans, blocking the early apoptotic events by targeting caspase-11 (or its human ortholog, caspase-5) represents a new possibility.

Of those genes exhibiting the highest statistical significant differential expressions in the submandibular glands of C57BL/6.NOD-*Aec1Aec2* mice at 8 weeks of age, which include *F8a* (factor VIII-associated gene A located within intron 22 and associated with Haemophilia A)[31] and *Cox-6a* (terminal enzyme of the mitochondrial electron transport chain that catalyzes the transfer of electrons from cytochrome *c* to oxygen and directly related to energy demand through neural activity or muscle adaptation/hormonal changes),[32] perhaps the more fascinating is *1700112L09Rik* encoding chimerin. Chimerin is a *Rac-1* repressor that, despite being overexpressed more than two-fold in the submandibular glands at 8 weeks, is strongly downregulated at 12 weeks of age, showing a direct relationship with an upregulation

in *Rac-1* expression. Rac1 is involved in signaling along several pathways, one involving PI3 K[33,34] and PKB (Akt)[35] and another involving MEKK1.[36] Both cascades are important regulators of a wide spectrum of biological processes, including cell proliferation, differentiation, apoptosis, lipid metabolism and coagulation. Not surprising, then, genes within these pathways, like *Mekk1*, *Mkk4, Map2k4*, *p38Mapk*, *Stat1* and *Elk-1* also showed an upregulated expression, even though not always reaching statistical significance. In addition, Rac1 is known to be important in cytoskeletal changes involving E-cadherin and catenin p120/Vav2[37] possibly indicative of glandular remodeling. Since these pathways can be regulated by factors of the TNF super family of genes, a serious question to be asked is whether any link between upregulation of *Rac-1* and any TNF-family proteins or receptors exists. This would once again focus attention on molecules encoded by *traf6*, *tnfip6* and *tnfaip1* that were upregulated at 8 weeks and downregulated at 12 weeks *vs traf3*, *tnfaip3*, *tnfrsf13c*, *tnfsf14* and *tnfrsf19* that were subsequently upregulated at 12 weeks. Also of interest is the reduced expression of *traf1* that occurs between 8 and 12 weeks of age (Figures 4 and 5). A loss of Traf1 levels would permit higher expression levels of NIP45, a transcription factor that potentiates NF-kB-driven expression of IL-4,[38] possibly explaining in part the important role IL-4 has been shown to play in development of SjS-like disease in NOD mice using IL-4 KO mice.[3,39]

One temporal inverse relationship worth investigating is that of *traf3 vs traf6* gene expression in the submandibular glands of C57BL/6.NOD-*Aec1Aec2* mice. As pointed out above, *traf6* gene expression is upregulated at 8 weeks, but downregulated at 12 weeks, whereas *traf3* gene expression is downregulated at 8 weeks and upregulated at 12 weeks. In a recent study, Häcker *et al*[40] provided evidence that these two TRAF molecules are involved in controlling diverse signaling pathways. For example, TRAF3 is essential for the induction of type 1 IFNs and the cytokine IL-10, most likely through the recruitment of TBK-1/NAK. Interestingly, our microarray data indicate that both *IL10ra* and *IL10rb* genes are upregulated at 12 weeks of age. In addition, TRAF3 appears to be an important downstream transduction signal for BAFF-BAFFR,[41] APRIL-BCMA,[42] CD70-CD27,[43] CD40L-CD40[41] and LIGHT-HVEM,[44] five systems thought to play a role in B lymphocyte hyper-reactivity of SjS. As early signs of an overt autoimmune attack against the submandibular glands of C57BL/6.NOD-*Aec1Aec2* mice can be observed by 12 weeks of age, including the appearance of leukocytes, it is important to note that three genes of the TNF superfamily, *tnfrsf19* (TAJ/TROY), *tnfrsf13* (BAFF receptor) and *tnfsf14* (LIGHT) were upregulated in the submandibular glands at 12 weeks as compared to 8 weeks of age, suggesting active signaling processes occurring within infiltrating immune cells, the salivary gland epithelial and/or neural cells *per se* (Figure 5). BAFF, for example, is known to regulate lymphocyte survival and activation.[45] BAFF binds to three receptors, BAFF receptor (BAFF-R), transmembrane activator and cytophilin ligand interactor (TACI), as well as B-cell maturation antigen (BCMA) known to be closely associated with the development of germinal-like centers in the salivary glands of SjS patients.[46,47] An upregulation of Nik, IKK and Nf-kB downstream of TACI and BCMA or Ppard, Cntn1, Poll and Dyrk1 associated with proliferation may account for the increased maturation and prolonged survival of B cells observed in both SjS patients and C57BL/6.NOD-*Aec1Aec2* mice. Interestingly, a recent microarray analysis on minor salivary glands derived from human SjS patients also found upregulated *BCMA* (*Tnfrsf17*)[48] consistent with our data from the mouse model. Similarly, LIGHT, which binds to the TR2 receptor of CD68-positive macrophages induces the phosphorylation of I*k*B and nuclear translocation of NF-kB.[49,50] One potential consequence of LIGHT signaling, as observed in rheumatoid arthritis,[50] might be the upregulation of matrix metalloprotease (MMP)-9 expression, and MMP9 has been shown to be actively induced in the submandibular glands of NOD mice during the disease state.[6,51] Lastly, an upregulation of *tnfrsf19* (Taj/TROY) focuses attention on neural tissue involvement, and studies suggest that the parasympathetic neural system along with the muscarinic acetylcholine type-3 receptor are targets of the autoimmune process.[16] Overall, then, while genes that are upregulated within the submandibular glands of C57BL/6.NOD-*Aec1Aec2* mice of 8 weeks of age tend to point to apoptotic events, those upregulated at 12 weeks of age point strongly to early immunoregulatory events.

Other genes that are highly expressed in the submandibular glands of C57BL/6.NOD-*Aec1Aec2* mice at 12 weeks of age include *Pde4b* and *Krt1*. Stimulation of TLR is known to upregulate *Pde4b* and production of PDE which, in turn, regulates intracellular levels of cAMP. Elevated intracellular cAMP has been associated with functional inhibition of numerous cell types such as lymphocytes, monocytes, macrophages, neutrophil, eosinophils, and mast cells.[52] Inhibitors of PDE4 have shown the ability to suppress the *in vitro* responses of cells involved in the inflammatory process;[52] however, only ablation of PDE4B impacted LPS signaling and TNF-α production, thereby demonstrating the highly specialized function of PDE4B in macrophages and its critical role in LPS signaling.[53] Thus, the upregulated expression of *Pde4b* by 12 weeks of age may indicate the appearance of functionally impaired macrophages, often suggested for the NOD mouse,[54] in the submandibular glands. Similarly, overexpression of *Krt1* (keratin) may be a compensatory process for the loss of acinar cells and may explain excessive keratosis observed in the cornea during the disease state.

In summary, these studies represent our initial attempt at using microarray technology to identify genes and gene clusters that may prove important in identifying underlying molecular mechanisms responsible for development of the physiological abnormalities, as well as regulating the autoimmune response, observed in the submandibular glands of C57BL/6.*NOD.Aec1Aec2* mice prior to onset of the clinical disease. Although these studies cover only about one-third of the mouse genome, we have identified to date both distinct signal transduction pathways and individual genes that, based on previous studies of the pathophysiological changes occurring in the submandibular glands, represent excellent candidates regulating development of SjS-like disease. These pathways (presented in Figures 3–5) suggest, when extrapolated, that there is an innate immunity that initiates an adaptive immunity favoring B lymphocyte activation. As we continue to mine the microarray data, it is now imperative to determine if such candidate genes and pathways are important or just our biased interpretation.

Acknowledgements

We thank Mr Jin Wang, Ms Grace Kim and Mr Eric Singson for their expert technical assistance. Supported in part by: PHS Grants DE014344 (ABP), DE015152 (ABP), DE55304 (ABP), U24 DE016509 (SC) from the NIH and the Sjögren's Syndrome Foundation (SC).

References

1 Jonsson R, Dowman SJ, Gordon T. Sjögren's syndrome. In: Koopman W (ed). Arthritis and Allied Conditions—A Textbook in Rheumatology, 15th edn. Lippincott Williams & Wilkins: Philadelphia, 2004, pp 1681–1705.
2 Brayer J, Lowry J, Cha S, *et al.* Alleles from chromosomes 1 and 3 of NOD mice combine to influence Sjogren's syndrome-like autoimmune exocrinopathy. J Rheumatol 2000;27:1896–1904.
3 Brayer JB, Cha S, Nagashima H, *et al.* IL-4-dependent effector phase in autoimmune exocrinopathy as defined by the NOD.IL-4-gene knockout mouse model of Sjogren's syndrome. Scand J Immunol 2001;54:133–140.
4 Cha S, Peck AB, Humphreys-Beher MG. Progress in understanding autoimmune exocrinopathy using the non-obese diabetic mouse: an update. Crit Rev Oral Biol Med 2002;13:5–16.
5 Robinson CP, Brayer J, Yamachika S, *et al.* Transfer of human serum IgG to nonobese diabetic Igmu null mice reveals a role for autoantibodies in the loss of secretory function of exocrine tissues in Sjogren's syndrome. Proc Natl Acad Sci USA 1998;95:7538–7543.
6 Yamachika S, Nanni JM, Nguyen KH, *et al.* Excessive synthesis of matrix metalloproteinases in exocrine tissues of NOD mouse models for Sjogren's syndrome. J Rheumatol 1998;25:2371–2380.
7 Humphreys-Beher MG, Peck AB. New concepts for the development of autoimmune exocrinopathy derived from studies with the NOD mouse model. Arch Oral Biol 1999;44(Suppl 1):S21–S25.
8 Cha S, Singson E, Cornelius J, *et al.* Muscarinic acetylcholine type-3 receptor desensitization due to chronic exposure to Sjogren's syndrome-associated autoantibodies. J Rheumatol 2006;33:296–306.
9 Humphreys-Beher MG, Hu Y, Nakagawa Y, *et al.* Utilization of the non-obese diabetic (NOD) mouse as an animal model for the study of secondary Sjogren's syndrome. Adv Exp Med Biol 1994;350:631–636.
10 Robinson CP, Yamachika S, Bounous DI, *et al.* A novel NOD-derived murine model of primary Sjogren's syndrome. Arthritis Rheum 1998;41:150–156.
11 Ishimaru N, Yoneda T, Saegusa K, *et al.* Severe destructive autoimmune lesions with aging in murine Sjogren's syndrome through Fas-mediated apoptosis. Am J Pathol 2000;156:1557–1564.
12 Groom J, Kalled SL, Cutler AH, *et al.* Association of BAFF/BLyS overexpression and altered B cell differentiation with Sjogren's syndrome. J Clin Invest 2002;109:59–68.
13 Robinson CP, Yamamoto H, Peck AB, *et al.* Genetically programmed development of salivary gland abnormalities in the NOD (nonobese diabetic)-scid mouse in the absence of detectable lymphocytic infiltration: a potential trigger for sialoadenitis of NOD mice. Clin Immunol Immunopathol 1996;79:50–59.
14 Ambrosetti A, Zanotti R, Pattaro C, *et al.* Most cases of primary salivary mucosa-associated lymphoid tissue lymphoma are associated either with Sjoegren syndrome or hepatitis C virus infection. Triple association between hepatitis C virus infection, systemic autoimmune diseases, and B cell lymphoma. Br J Haematol 2004;126:43–49.
15 Cha S, van Blockland SC, Versnel MA, *et al.* Abnormal organogenesis in salivary gland development may initiate adult onset of autoimmune exocrinopathy. Exp Clin Immunogenet 2001;18:143–160.
16 Nguyen KH, Brayer J, Cha S, *et al.* Evidence for antimuscarinic acetylcholine receptor antibody-mediated secretory dysfunction in nod mice. Arthritis Rheum 2000;43:2297–2306.
17 Gao J, Cha S, Jonsson R, *et al.* Detection of anti-type 3 muscarinic acetylcholine receptor autoantibodies in the sera of Sjogren's syndrome patients by use of a transfected cell line assay. Arthritis Rheum 2004;50:2615–2621.
18 Cavill D, Waterman SA, Gordon TP. Antibodies raised against the second extracellular loop of the human muscarinic M3 receptor mimic functional autoantibodies in Sjogren's syndrome. Scand J Immunol 2004;59:261–266.
19 Dawson LJ, Field EA, Harmer AR, *et al.* Acetylcholine-evoked calcium mobilization and ion channel activation in human labial gland acinar cells from patients with primary Sjogren's syndrome. Clin Exp Immunol 2001;124:480–485.
20 Li J, Ha YM, Ku NY, *et al.* Inhibitory effects of autoantibodies on the muscarinic receptors in Sjogren's syndrome. Lab Invest 2004;27:27.
21 Yui MA, Muralidharan K, Moreno-Altamirano B, *et al.* Production of congenic mouse strains carrying NOD-derived diabetogenic genetic intervals: an approach for the genetic dissection of complex traits. Mamm Genome 1996;7:331–334.

22 Chesnut K, She JX, Cheng I, *et al.* Characterizations of candidate genes for IDD susceptibility from the diabetes-prone NOD mouse strain. Mamm Genome 1993;4:549–554.
23 Cha S, Nagashima H, Brown VB, *et al.* Two NOD Idd-associated intervals contribute synergistically to the development of autoimmune exocrinopathy (Sjogren's syndrome) on a healthy murine background. Arthritis Rheum 2002;46:1390–1398.
24 Takeichi M. Cadherin cell adhesion receptors as a morphogenetic regulator. Science 1991;251:1451–1455.
25 Eckenrode SE, Ruan Q, Yang P, *et al.* Gene expression profiles define a key checkpoint for type 1 diabetes in NOD mice. Diabetes 2004;53:366–375.
26 Humphreys-Beher MG, Peck AB, Dang H, *et al.* The role of apoptosis in the initiation of the autoimmune response in Sjogren's syndrome. Clin Exp Immunol 1999;116:383–387.
27 Schauvliege R, Vanrobaeys J, Schotte P, *et al.* Caspase-11 gene expression in response to lipopolysaccharide and interferon-gamma requires nuclear factor-kappa B and signal transducer and activator of transcription (STAT) 1. J Biol Chem 2002;277:41624–41630 (E-pub 42002 Aug 41626).
28 Robinson CP, Yamachika S, Alford CE, *et al.* Elevated levels of cysteine protease activity in saliva and salivary glands of the nonobese diabetic (NOD) mouse model for Sjogren syndrome. Proc Natl Acad Sci USA 1997;94:5767–5771.
29 Gu Y, Kuida K, Tsutsui H, *et al.* Activation of interferon-gamma inducing factor mediated by interleukin-1beta converting enzyme. Science 1997;275:206–209.
30 Cha S, Brayer J, Gao J, *et al.* A dual role for interferon-gamma in the pathogenesis of Sjogren's syndrome-like autoimmune exocrinopathy in the nonobese diabetic mouse. Scand J Immunol 2004;60:552–565.
31 Peters MF, Ross CA. Isolation of a 40-kDa Huntingtin-associated protein. J Biol Chem 2001;276:3188–3194 (E-pub 2000 October 3116).
32 Ongwijitwat S, Wong-Riley MT. Functional analysis of the rat cytochrome c oxidase subunit 6A1 promoter in primary neurons. Gene 2004;337:163–171.
33 Rodriguez-Viciana P, Warne PH, Khwaja A, *et al.* Role of phosphoinositide 3-OH kinase in cell transformation and control of the actin cytoskeleton by Ras. Cell 1997;89:457–467.
34 Lee HY, Srinivas H, Xia D, *et al.* Evidence that phosphatidylinositol 3-kinase- and mitogen-activated protein kinase kinase-4/c-Jun NH2-terminal kinase-dependent Pathways cooperate to maintain lung cancer cell survival. J Biol Chem 2003;278:23630–23638 (E-pub 22003 April 23624).
35 Qian Y, Zhong X, Flynn DC, *et al.* ILK mediates actin filament rearrangements and cell migration and invasion through PI3K/Akt/Rac1 signaling. Oncogene 2005;24:3154–3165.
36 Uhlik MT, Abell AN, Cuevas BD, *et al.* Wiring diagrams of MAPK regulation by MEKK1, 2, and 3. Biochem Cell Biol 2004;82:658–663.
37 Natale DR, Watson AJ. Rac-1 and IQGAP are potential regulators of E-cadherin-catenin interactions during murine preimplantation development. Gene Expr Patterns 2002;2:17–22.
38 Bryce PJ, Oyoshi MK, Kawamoto S, *et al.* TRAF1 regulates Th2 differentiation, allergic inflammation and nuclear localization of the Th2 transcription factor, NIP45. Int Immunol 2006;18:101–111 (E-pub 2005 December 2013).
39 Gao J, Killedar S, Cornelius JG, *et al.* Sjogren's syndrome in the NOD mouse model is an interleukin-4 time-dependent, antibody isotype-specific autoimmune disease. J Autoimmun 2006;26:90–103 (E-pub 2006 January 2018).
40 Hacker H, Redecke V, Blagoev B, *et al.* Specificity in Toll-like receptor signalling through distinct effector functions of TRAF3 and TRAF6. Nature 2006;439:204–207 (E-pub 2005 November 2023).
41 Ni CZ, Oganesyan G, Welsh K, *et al.* Key molecular contacts promote recognition of the BAFF receptor by TNF receptor-associated factor 3: implications for intracellular signaling regulation. J Immunol 2004;173:7394–7400.
42 Hatzoglou A, Roussel J, Bourgeade MF, *et al.* TNF receptor family member BCMA (B cell maturation) associates with TNF receptor-associated factor (TRAF) 1, TRAF2, and TRAF3 and activates NF-kappa B, elk-1, c-Jun N-terminal kinase, and p38 mitogen-activated protein kinase. J Immunol 2000;165:1322–1330.
43 Yamamoto H, Kishimoto T, Minamoto S. NF-kappaB activation in CD27 signaling: involvement of TNF receptor-associated factors in its signaling and identification of functional region of CD27. J Immunol 1998;161:4753–4759.
44 Hauer J, Puschner S, Ramakrishnan P, *et al.* TNF receptor (TNFR)-associated factor (TRAF) 3 serves as an inhibitor of TRAF2/5-mediated activation of the noncanonical NF-kappaB pathway by TRAF-binding TNFRs. Proc Natl Acad Sci USA 2005;102:2874–2879 (E-pub 2005 February 2811).
45 Schneider P. The role of APRIL and BAFF in lymphocyte activation. Curr Opin Immunol 2005;17:282–289.
46 Lavie F, Miceli-Richard C, Quillard J, *et al.* Expression of BAFF (BLyS) in T cells infiltrating labial salivary glands from patients with Sjogren's syndrome. J Pathol 2004;202:496–502.
47 Mariette X, Roux S, Zhang J, *et al.* The level of BLyS (BAFF) correlates with the titre of autoantibodies in human Sjogren's syndrome. Ann Rheum Dis 2003;62:168–171.
48 Hjelmervik TO, Petersen K, Jonassen I, *et al.* Gene expression profiling of minor salivary glands clearly distinguishes primary Sjogren's syndrome patients from healthy control subjects. Arthritis Rheum 2005;52:1534–1544.
49 Bobik A, Kalinina N. Tumor necrosis factor receptor and ligand superfamily family members TNFRSF14 and LIGHT: new players in human atherogenesis. Arterioscler Thromb Vasc Biol 2001;21:1873–1875.
50 Kim WJ, Kang YJ, Koh EM, *et al.* LIGHT is involved in the pathogenesis of rheumatoid arthritis by inducing the expression of pro-inflammatory cytokines and MMP-9 in macrophages. Immunology 2005;114:272–279.
51 Azuma M, Aota K, Tamatani T, *et al.* Suppression of tumor necrosis factor alpha-induced matrix metalloproteinase 9 production in human salivary gland acinar cells by cepharanthine occurs via downregulation of nuclear factor kappaB: a possible therapeutic

agent for preventing the destruction of the acinar structure in the salivary glands of Sjogren's syndrome patients. Arthritis Rheum 2002;46:1585–1594.

52 Teixeira MM, Gristwood RW, Cooper N, *et al.* Phosphodiesterase (PDE)4 inhibitors: anti-inflammatory drugs of the future? Trends Pharmacol Sci 1997;18: 164–171.

53 Jin SL, Lan L, Zoudilova M, *et al.* Specific role of phosphodiesterase 4B in lipopolysaccharide-induced signaling in mouse macrophages. J Immunol 2005;175: 1523–1531.

54 Serreze DV. Autoimmune diabetes results from genetic defects manifest by antigen presenting cells. FASEB J 1993;7:1092–1096.

Supplementary Information accompanies the paper on the Laboratory Investigation website (http://www.nature.com/labinvest)